Available online at www.sciencedirect.com

ScienceDirect

Procedia CIRP 115 (2022) 18–23

www.elsevier.com/locate/procedia

10th CIRP Global Web Conference – Material Aspects of Manufacturing Processes

Exploring the Applicability of Sinterjoining to Combine Additively Manufactured Ceramic Components

Johannes Schubert[a,*], Yannik End[a], Volker Schulze[a], Frederik Zanger[a]

[a]*Karlsruhe Institute of Technology (KIT), wbk Institute of Production Science, Kaiserstraße 12, 76131 Karlsruhe, Germany*

* Corresponding author. Tel.: +49 1523 950 2658; fax: +49 721 608 45004. *E-mail address:* johannes.schubert@kit.edu

Abstract

This paper examines the general applicability of sinterjoining for combining the advantages of Ceramic Injection Molding (CIM) and Additive Manufacturing (AM) as well as different AM processes. To do so, the geometric tolerance, the pre-sintering temperature and the co-sintering time are varied exemplarily on samples produced by vat photopolymerization (VPP) to minimize the force required for inserting the bodies and to maximize the degree of sintering. The results show that degrees of sintering larger 90 % can be obtained reproducibly. Thus, sinterjoining can be considered as a promising approach for combining the advantages of several ceramic manufacturing processes.

© 2022 The Authors. Published by Elsevier B.V.
This is an open access article under the CC BY-NC-ND license (https://creativecommons.org/licenses/by-nc-nd/4.0)
Peer-review under responsibility of the scientific committee of the 10th CIRP Global Web Conference –Material Aspects of Manufacturing Processes (CIRPe2022)

Keywords: Additive Manufacturing (AM), Vat Photopolymerization (VPP), SinterJoining, Ceramics, Aluminum Oxide (Al_2O_3)

1. Introduction

The demands on ceramic components are continuously increasing [1]. Ceramic Injection Molding (CIM) allows the efficient production of ceramic components in large quantities. Somehow, the achievable design complexity and the individualization of components is strongly limited [1,2]. In contrast, Additive Manufacturing (AM) offers enormous design freedom. Furthermore, no dedicated tools are required for building up the components. Therefore, the individualization of components is easily possible. However, the productivity of AM processes is very low, compared to CIM [1,3]. Furthermore, different AM processes have distinct advantages and lead to different component properties [3,4]. Therefore, combining CIM and an additive manufacturing process, as well as different AM processes seem to be promising approaches for efficiently manufacturing complex and individualized components.

Approaches for joining ceramic components are active metal brazing and the use of adhesives, e.g.. Generally, the auxiliary materials used thereby limit the component properties, e.g. in terms of their strength or their high temperature applicability [5]. One approach to join powder-metallurgically prepared components without auxiliary materials is sinterjoining. This concept is for ceramics just barely investigated, especially in the context of additive manufacturing [6,7]. Therefore, the aim of this research is to examine the general applicability of sinterjoining for connecting additively manufactured ceramic components.

2. Materials and methods

2.1. Sinterjoining

In sinterjoining, green or brown parts are joined in a common sintering process based on identical or different volume shrinkage. Alternatively, the joining of a green or

2212-8271 © 2022 The Authors. Published by Elsevier B.V.
This is an open access article under the CC BY-NC-ND license (https://creativecommons.org/licenses/by-nc-nd/4.0)
Peer-review under responsibility of the scientific committee of the 10th CIRP Global Web Conference –Material Aspects of Manufacturing Processes (CIRPe2022)
10.1016/j.procir.2022.10.043

brown part and a sintered part is generally possible. To do so, the parts are precisely positioned inside each other before a subsequent sintering process is leading to the intended material connection [8-10]. In a first process variant, both parts exhibit the same volume shrinkage. To facilitate a material connection between both parts, the contact surfaces have to be precisely adjusted to maintain a sufficient contact during the whole sintering process [8]. In a second process variant, the outer part exhibits a larger volume shrinkage than the inner part. This is leading to an additional press-fit connection improving the material connection and increasing the reproducibility of the joining process [8,10,11].

To investigate the general applicability of sinterjoining for combining additively manufactured ceramic components, the second approach seems to be more appropriate, based on the additional press-fit in the joining area. Therefore, the second concept was used as the basis for the research in this paper.

For investigating the general applicability, the individual parts were built from the same material (see Sect. 2.2). Thus, additional influences could be largely eliminated. Nevertheless, to achieve different shrinkages in the inner and outer part, a pre-sintering step was carried out for the inner part leading to a first volume shrinkage. This is transforming the press fit into a clearance fit connection, allowing the positioning of both parts inside each other. In the subsequent co-sintering step, the material connection was created by the larger remaining volume shrinkage of the outer part. In total, this results in the process chain shown in Fig. 1.

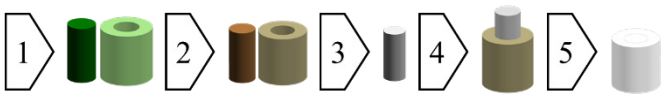

Fig. 1. Schematic process chain of sinterjoining applied in this paper:
(1) additive manufacturing of green parts by vat photopolymerization,
(2) thermal debinding of inner and outer part,
(3) pre-sintering of the inner part leading to initial volume shrinkage,
(4) precise positioning of inner and outer part inside each other,
(5) co-sintering of both parts leading to material connection.

2.2. Additive Manufacturing of the green parts

The manufacturing of the green parts was carried out by vat photopolymerization comprising a LED light source (VPP-LED) on the printer CeraFab 7500 (Lithoz GmbH, Vienna, Austria). Compared to other additive manufacturing processes, VPP provides high geometric precision and excellent surface qualities [3], which makes this process ideally suited for investigating sinterjoining of ceramics. LithaLox 350 (Lithoz GmbH, Vienna, Austria) was used as the ceramic slurry for VPP. It consists of high-purity aluminum oxide (Al_2O_3) and the photosensitive binder required for shaping. By choosing the widely used standard ceramic Al_2O_3, a broad transferability of the results should be facilitated. For printing, the exposure parameters listed in Table 1 were applied. To improve the adhesion of the green parts on the building platform, the exposure time was slightly increased compared to the recommended standard parameters [12].

Table 1. Summary of the exposure parameters applied for VPP.

parameter	starting layer	general layer
exposure intensity in mW/cm²	40.7	40.7
exposure time in s	4.9	4.3
exposure energy in mJ/cm²	200	175

Cylinders and sleeves with a height of 10 mm were used as test specimens. The outer diameter of the sleeves was 10 mm. The inner diameter of the sleeves and the outer diameter of the cylinders were varied in 6 steps in the range of 4.8 to 5.0 mm and in 5 steps in the range of 5.04 to 5.2 mm, respectively, to check the limitations of sinterjoining. The resulting step size of 40 µm corresponds to the pixel grid of the VPP system. A finer step size is not possible with the DLP projector used in the CeraFab 7500 printer. All cylinder sizes were combined with all sleeve sizes, due to the unknown shrinkage behavior during debinding and pre-sintering. This set of in total 30 combinations is defined as one series of test specimens. To efficiently examine the suitability of sinterjoining and to identify fundamental dependencies, a large number of parameter combinations were performed just once.

The used VPP process requires the deposition of a full-surface adhesive layer on the build platform with increased exposure energy. In order to prevent the adhesive layer and the potentially resulting fillet caused by adhering slurry (see Fig. 2a in red) from influencing the sintering process, the cylinder and sleeve edges were rounded in CAD with a rounding radius of 0.2 mm. These fillets can be filled with adhering slurry without negative influence on the joining result (see Fig. 2b). In addition, this results in a minimal lead-in chamfer for the initial centering of the components.

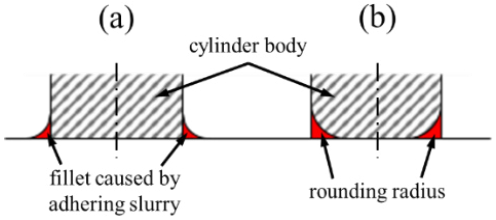

Fig. 2. Schematic depiction of the optimization of the cylinder geometry
(a) initial geometry with fillets caused by adhering slurry
(b) optimized geometry with rounding radius.

To ensure precise alignment of the components and to minimize or at least standardize the influence of the slicer integrated in the machine software, the concept of the so-called bounding box was employed. This involves a bounding box structure being created in CAD with the exact dimensions of the printing area. The corners of this box are defined by (inverted) pixels. Because of the same dimensions of bounding box and printing area, the slicer always positions the box exactly at the corner of the pixel grid, and the alignment of the individual components can be carried out precisely in CAD. Based on the pixel grid of 40 µm edge length, the components are always aligned in intervals of integer multiples of 40 µm (see Fig. 3) [14]. This ensures the highest possible precision of the components.

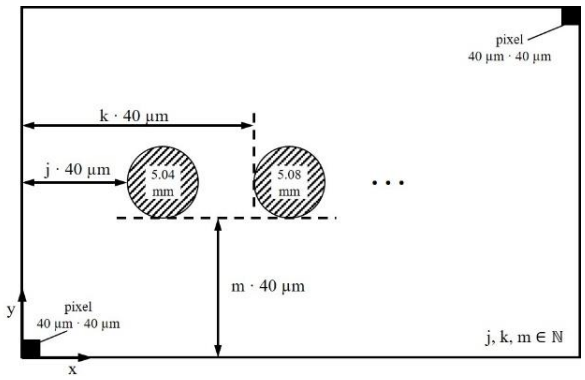

Fig. 3. Schematic depiction of the bounding box concept for optimizing the positioning the parts on the building platform (not true to scale).

After printing, the parts were separated from the building platform by a razor blade and cleaned manually in a bath of isopropanol. The components were then dried for at least 24 h in a drying chamber (Totech Superdry SD, Totech Europe BV, Zwolle, Netherlands) at 40 °C. This removed the superficial residual moisture from the components, thus improving their further handling.

To guarantee sufficient dimensional accuracy of all components, a full inspection of the outer and inner diameters of the cylinders and sleeves in the green state was carried out by an outside micrometer (Micromar 40 ER, Mahr GmbH, Göttingen, Germany) and an inside micrometer (MMO Messmittelonline Measuring Instruments, Kloster-Lenin, Germany), respectively. To do so, three measurements of the diameter of each sample were carried out at different positions along the circumference and the mean value was calculated. The accuracy of the measurement via micrometers was confirmed by detailed comparative measurements on reference parts by a coordinate measuring machine (Zeiss Prismo KMG, Carl Zeiss IQS Deutschland GmbH, Oberkochen, Germany). Here, the roundness and cylindricity of the components were also quantified.

2.3. Debinding

Subsequent debinding was carried out according to the safety program in the slurry data sheet [15] with the temperature curve shown in Table 2 in ambient air (Carbolite GLO, Carbolite Gero GmbH & Co. KG, Neuhausen, Germany). The debinding behavior was examined by thermogravimetric analysis (TGA) of a disk (diameter 6 mm, thickness 2 mm) carried out on a STA 449 F1 Jupiter (Netzsch-Gerätebau GmbH, Selb, Germany) in ambient air with a heating rate of 0.5 K/min. Due to the small sample, the time delay in debinding, i.e. the time required for the binder to reach the surface of the sample, could be mainly eliminated. After debinding, the inner diameter of the sleeves was measured again with an inside micrometer.

Table 2. Debinding temperature profile.

step	heating time in min	heating rate in K/min	end temperature in °C	dwell time in min
0			25	
1	190	0.5	120	60
2	100	0.1	130	240
3	400	0.1	170	240
4	500	0.1	220	240
5	300	0.1	250	360
6	750	0.1	325	360
7	525	0.2	430	120
8	670	1.0	1100	0
9	1070	-1.0	30	0

2.4. Sintering

According to the slurry data sheet, sintering at 1700 °C and a holding time of 2 h is recommended [15]. In order to convert the interference fit into a clearance fit, a volume shrinkage of the cylinders is required. This was realized by pre-sintering the cylinders. On the one hand, a sufficiently large volume shrinkage is necessary for placing the components into each other. On the other hand, an excessive anticipated shrinkage, resulting in a large shrinkage difference between the cylinder and the sleeve in the final sintering step, can impair the joining quality and possibly also lead to cracks and other defects. Therefore, the influence of the pre-sintering temperature, especially in combination with the geometric offset, was of major interest. Thus, pre-sintering took place at 1300 °C and 1400 °C with the temperature profiles shown in Table 3. The individual steps correspond to the recommended specifications in the slurry data sheet [15], except the adjustment of the sintering temperature itself.

Table 3. Pre-sintering temperature profile.

step	heating time in min	heating rate in K/min	end temperature in °C	dwell time in min
0			25	
1	60	2.9	200	0
2	600	0.67	600	0
3	360	1.53	1150	0
4	172[a] | 285[b]	0.88	1300[a] | 1400[b]	240
5	120[a] | 240[b]	-0.83	1200	0
6	628	-1.83	50	0

[a]profile for end temperature 1300 °C, [b]profile for end temperature 1400 °C,

After pre-sintering, the outer diameter of the sleeves was measured with an outside micrometer. Then, the sleeves were matched to the corresponding sleeve and inserted into each other manually. The insertability was evaluated in 3 classes based on the force required:

a) no additional force required beyond gravity
b) force required for insertion, i.e. pressure applied by the thumb
c) no insertion at all possible

The final sintering step took place with the recommended temperature profile at 1700 °C for 2 h in ambient air (Carbolite HTF, Carbolite GmbH & Co. KG, Neuhausen, Germany). Furthermore, the dwell time, i.e. the holding time, at 1700 °C

was increased to 6 h in an additional study (see Table 4). The heating time, i.e. the time required to reach to corresponding temperature level, was kept unchanged compared to [15].

Table 4. Sintering temperature profile.

step	heating time in min	heating rate in K/min	end temperature in °C	dwell time in min
0			25	
1	60	2.9	200	0
2	600	0.67	600	0
3	360	1.53	1150	0
4	627	0.88	1700	120 | 360
5	600	-0.83	1200	0
6	628	-1.83	50	0

he influence of the pre-sintering and sintering parameters was investigated in a full factorial test plan shown in Table 5. The nomenclature introduced there will be used in the following for easier identification of the samples. Each test series was performed with one series of samples, i.e. 30 combinations of cylinders and sleeves per parameter combination.

Table 5. Factor levels and nomenclature of the full factorial test plan.

		dwell time at 1700°C	
		120 min	360 min
pre-sintering temperature	1300 °C	series I	series II
	1400 °C	series III	series IV

After sintering, the samples were prepared materialographically. For this, 2 mm were ground off the lower end of the specimens, offering a view into the interior of the component. The evaluation of the joining quality was performed based on the Degree of Sintering (DoS) by manual image analysis in the software imageJ. This value represents the proportion of the sintered interface in relation to the total interface between cylinder and sleeve. In the specific case of the circular interface, the calculation is performed on the basis of the sintered circular sections using Fig. 4 and Formula 1.

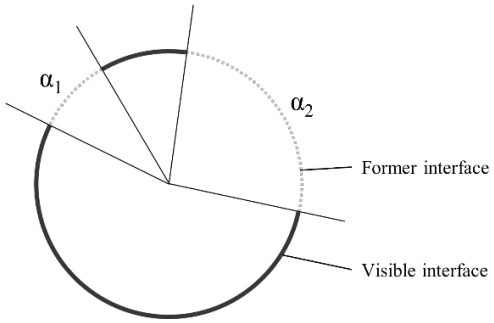

Fig. 4. Schematic visualization of Degree of Sintering for a circular interface.

$$Degree\ of\ Sintering\ (DoS) = \frac{\sum \alpha_i}{360°} \quad (1)$$

3. Results

3.1. Dimensional analysis of the green parts

The results of measuring the green bodies are exemplarily shown for cylinders of different diameters in Table 6.

Table 6. Diameter of the cylinder parts in green state demonstrating the accuracy of the used VPP process (series I to IV).

target diameter in mm	measured mean value in mm	deviation in mm	standard deviation in mm
5.040	5.033	-0.007	0.008
5.080	5.072	-0.008	0.006
5.120	5.116	-0.004	0.005
5.160	5.142	-0.018	0.008
5.200	5.194	-0.006	0.006

All deviations are within the edge length of half a pixel, i.e. 20 µm. Increasing the slightly too small cylinders by one pixel would cause a larger magnitude of oversize.

Reference measurements by a coordinate measuring machine on four cylinders with target diameter 5.120 mm showed a diameter of 5.108 mm with a standard deviation of 0.004 mm. The only small deviations of the values measured by the micrometer compared to the coordinate measuring machine confirmed the accuracy of the micrometer. Measurements of roundness and cylindricity on 4 randomly selected cylinders and 4 randomly selected sleeves yielded values of 0.020 mm and 0.023 mm for the cylinders as well as 0.018 mm and 0.030 mm for the sleeves. All standard deviations are below 0.005 mm. Based on the measured values regarding diameter, roundness and cylindricity, a further improvement in accuracy of the green parts is not feasible.

3.2. Debinding

The debinding curve of the small disk measured in the TGA analysis is shown in Fig. 5.

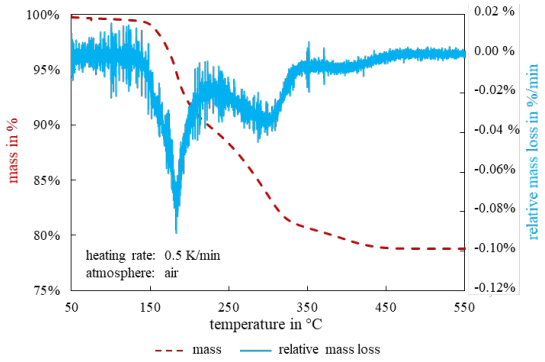

Fig. 5. Thermogravimetric analysis of the debinding of VPP green parts.

Accordingly, the actual debinding process takes place in stages up to 450 °C. Above a temperature of 450 °C, no further mass loss occurs. This confirms the values given in the slurry data sheet [15] and in Table 2. The deviation from 430 °C in the debinding profile to 450 °C in the TGA can be attributed to the continuous heating in the TGA measurement and the resulting time delay. Whilst the binder is still diffusing to the surface of the sample, the oven continues to heat at a constant rate of 0.5 K/min, which means that a loss of mass remains measurable even at higher temperatures.

The further temperature increase up to 1100 °C in the debinding temperature profile results in a first sintering of the components, which increases the brown strength of the

cylinders and sleeves. This is required for damage-free handling and insertion of the components into each other.

3.3. Inserting cylinder and sleeve

Table 7 summarizes the inner diameters of the sleeves in their debindered and of the cylinders in their pre-sintered state in mm, respectively. Furthermore, the corresponding standard deviation (SD) is shown. In this states, the cylinder and sleeve are inserted into each other. It can be seen that pre-sintering at 1400 °C leads to an additional average volume shrinkage of 174 µm compared to pre-sintering at 1300 °C. At the same time, the low standard deviation shows that the debinding and sintering steps were conducted very consistently. To enable the cylinder and sleeve to fit together, the inner diameter of the sleeve must be larger than the outer diameter of the cylinder, i.e. a clearance fit. Based on the values in Table 7, preliminary statements can therefore already be made about the suitability of cylinder and sleeve.

Experimental insertion of sleeves and cylinders pre-sintered at 1300 °C (i.e. series I and II) show that they do not fit in any of the combinations considered. This is in line with the values shown in Table 7. Even the smallest cylinder with 4.819 mm is still 32 µm bigger than the largest sleeve with 4.787 mm. Due to the interference, no insertion is possible. Consequently, no investigation of the common sintering can be performed for any of the cylinders pre-sintered at 1300 °C (test series I and II).

Table 7. Diameters and standard deviation (SD) of sleeves and cylinders in their matching state in mm (series I to IV).

	target dimension	debindered		pre-sintered at 1300 °C		pre-sintered at 1400 °C	
	green state	mean	SD	mean	SD	mean	SD
sleeve	4.80	4.612	0.019				
	4.84	4.652	0.010				
	4.88	4.679	0.008				
	4.92	4.705	0.008				
	4.96	4.741	0.012				
	5.00	4.787	0.019				
cylinder	5.04			4.819	0.005	4.649	0.012
	5.08			4.857	0.007	4.686	0.012
	5.12			4.901	0.006	4.725	0.006
	5.16			4.934	0.004	4.756	0.008
	5.20			4.979	0.004	4.801	0.008

Table 8 shows the results of matching cylinders and sleeves of test series III and IV, i.e. pre-sintered at 1400 °C. The results correspond to the expectations based on the measurement of the parts (see Table 7). If the outer diameter of the cylinders is significantly smaller than the inner diameter of the sleeves, gravity is sufficient to place cylinders and sleeves into each other. A clearance of about 30 µm is shown to be the limiting value. If the clearance is smaller, an additional force is required for inserting the cylinders. This can be attributed to the friction between cylinder and sleeve as well as possible local deviations in the diameter or roundness of the components. If the outside diameter of the cylinders is larger than the inside diameter of the sleeves, fitting together is not possible. A comparison of the dimensions in the green state shows that up to an oversize of approx. 4 % the cylinders shrink sufficiently far at 1400 °C and a dwell time of 2 h to be insertable into the debindered sleeves.

Table 8. Compatibility of cylinders and sleeves pre-sintered at 1400 °C (series III and IV), based on their dimension in the green state.

	green dimension	cylinders, pre-sintered at 1400 °C				
		5.04	5.08	5.12	5.16	5.20
sleeve	4.80	c	c	c	c	c
	4.84	b	c	c	c	c
	4.88	a	c	c	c	c
	4.92	a	b	c	c	c
	4.96	a	a	b	c	c
	5.00	a	a	a	b	c

[a]no additional force required beyond gravity, [b]force required for insertion, [c]no insertion possible at all

3.4. Degree of Sintering

Fig. 6 shows exemplarily micrographs of samples after the final sintering step. In Figs. 6a and 6c, the specimens are shown in their as prepared state. In Fig. 6b and 6d, the interface between cylinder and sleeve is indicated for comparison. In Fig. 6a und 6b, the sample consisting of a 5.04 mm cylinder and a 5.00 mm sleeve sintered for 120 minutes (series III) is shown. The initial oversize of 0.8 % is leading to a Degree of Sintering (DoS) of 41 %. In comparison, Fig. 6b and 6d show the sample consisting of a 5.12 mm cylinder and a 4.96 mm sleeve sintered for 360 minutes (series IV). The initial oversize of 3.2 % is leading to a DoS of 92 %. The enlarged sections illustrate the difference between the specimens due to the enlarged interface?

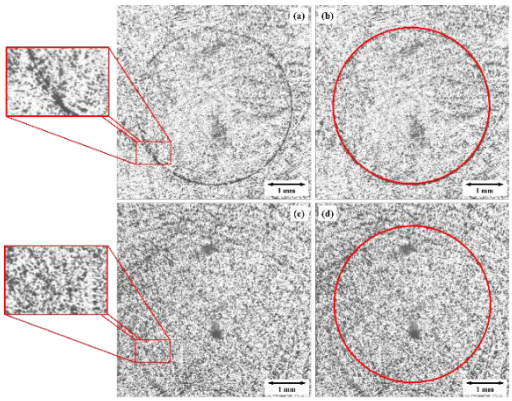

Fig. 6. Micrographs of samples after the final sintering step:
(a) and (b) series III sample 5.04/5.00 (cylinder/sleeve) with DoS of 41 %,
(c) and (d) series IV sample 5.12/4.96 with DoS of 92 %;
(a) and (c) show the images in the as-prepared state,
(b) and (d) additionally include an indication of the original interface.

An overview of the degrees of sintering in relation to the green part dimensions and the dwell time is given in Table 9. It can be seen that, in general, larger oversizes of cylinder and sleeve lead to higher degrees of sintering. Here, sintering degrees of 90 % could be achieved several times. This tendency is generally independent of the dwell time, although an extension of the dwell time from 120 to 360 minutes leads to a lower effect of the oversize and thus, to lower differences in the DoS. Overall, an extension of the dwell time can homogenize the values and increase the reproducibility.

Although, the highest degrees of sintering could be achieved at dwell times of 2 h. However, this can also be attributed to the comparatively local observation in a micrograph at a specific position of the sample. These comparatively small difference should therefore not be attributed too much significance.

A noteworthy change in the microstructure or pore distribution due to the longer dwell time could not be detected. It is noticeable that in some specimens (irrespective of the holding time) a circular arrangement of the pores, which are dark in Fig. 6, can be seen. This can probably be attributed to the debinding process, in which the binder diffuses outward along the shortest path to the surface.

By considering the results of the joinability after pre-sintering, a conflict of interest arises. On the one hand, the oversize may not be too large to allow the components to be fitted together. The limit value here is about 4 %. On the other hand, a larger oversize in the green state leads to higher degrees of sintering. Therefore, a satisfactory compromise must be found.

Table 9. Degree of Sintering of the samples of test series III and IV in %.

		cylinder									
		series III (2 h dwell time)					series IV (6 h dwell time)				
	green dimension	5.04	5.08	5.12	5.16	5.20	5.04	5.08	5.12	5.16	5.20
sleeve	4.80	-	-	-	-	-	-	-	-	-	-
	4.84	94	-	-	-	-	90	-	-	-	-
	4.88	83	-	-	-	-	80	-	-	-	-
	4.92	80	82	-	-	-	80	90	-	-	-
	4.96	64	73	86	-	-	80	84	92	-	-
	5.00	41	67	72	96	-	80	81	84	86	-

4. Conclusion and outlook

In this work, the applicability of sinterjoining to combine additively manufactured ceramic parts was investigated. First, the printing accuracy and reproducibility were optimized and quantified by applying the bounding box concept. On the basis of cylinders and sleeves with different geometric dimensions, a multi-stage process of pre-sintering the cylinders, inserting them into the debindered sleeves and common final sintering was investigated. The following results were obtained:

- In principle, sinterjoining of ceramic VPP components can be realized with the process chain described above. This process chain can therefore combine the advantages of AM and CIM as well as various AM processes for an efficient production.
- Pre-sintering the cylinders at 1300 °C for 2 h is not sufficient to transform an interference of 0.8 % in the green state into a clearance fit in the brown / pre-sintered state.
- Up to an oversize of approx. 4 %, pre-sintering at 1400 °C for 2 h leads to a sufficient clearance fit.
- The bigger the oversize in the green state, the higher the degree of sintering of the joined component.
- A compromise between insertability and Degree of Sintering has to be found.
- An extension of the dwell time in the combined sintering step tends to lead to more uniform results without influencing the microstructure and pore distribution, respectively.

The results of this publication provide a starting point for detailed investigation. In addition to a further optimization of the process parameters, a transfer to other interface geometries, e.g. oval, angular, polygonal, is planned. Likewise, the combination of different materials in a component is to be investigated, whereby the component properties can be specifically adapted to the requirements. Simulation of the sintering behavior can be of considerable support here.

Acknowledgements

The authors would like to thank Stephan Laube, Institute for Applied Materials – Materials Science and Engineering at Karlsruhe Institute of Technology (KIT) for performing the thermogravimetric measurements.

References

[1] Michaelis A, Scheithauer U, Moritz T, Weingarten S, Abel J, Schwarzer E, Kunz W. Advanced Manufacturing for Advanced Ceramics. Procedia CIRP, 2020; 95:18-22.
[2] Von Witzleben M, Hajek K, Raab D. Spritzgießen. In: Kollenberg W, editor. Technische Keramik. Essen: Vulkan Verlag; 2018. p. 470-478.
[3] Kollenberg W. Additive Fertigung keramischer Komponenten. Essen: Vulkan-Verlag; 2020.
[4] Travitzky N, Bonet A, Dermeik B, Frey T, Filbert-Demut I, Schlier L, Schlordt T, Greil P. Additive Manufacturing of Ceramic-Based Materials. Advanced Engineering Materials, 2014; 16,6,729-754.
[5] Tillmann W. Fügen. In: Kollenberg W, editor. Technische Keramik. Essen: Vulkan Verlag; 2018. p. 542-554.
[6] Ruh A, Dieckmann AM, Heldele R, Piotter V, Ruprecht R, Munzinger C, Fleischer J, Haußelt J. Production of two-material micro-assemblies by two-component powder injection molding and sinter-joining. Microsystem Technologies 2008;14:1805.
[7] Ruh A, Klimascha K, Piotter V, Plewa K, Ritzhaupt-Kleissl HJ, Fleischer J. The development of two-component micro powder injection moulding and sinter joining. Microsystem Technologies 2011;17:1547.
[8] Klimscha K. Einfluss des Fügespalts auf die erreichbare Verbindungsqualität beim Sinterfügen. Dissertation, Kalsruher Institut für Technologie (KIT); 2014.
[9] Kolaska H. Innovative und wirtschaftliche Bauteile durch Pulvermetallurgie. Düsseldorf: VDI-Verlag; 1993.
[10] Esper FJ. Pulvermetallurgie, das flexible und fortschrittliche Verfahren für wirtschaftliche und zuverlässige Bauteile. Renningen-Malmsheim: expert Verlag, Band 494; 1996.
[11] Huber A. Sinterfügen von Stahl und Hartmetall. Dissertation, Karlsruher Institut für Technologie (KIT); 2011
[12] Lithoz GmbH. Material Process Parameters, Material: LithaLox 350, Geometry: Demo Screw, Data Sheet. Vienna; 2019.
[13] Zhang SX, Li QF, Ho MK, Tong KK. Sinter bonding sticks MIM ahead again. In: Technical Paper, metal-powder.net. Kidlington: Elsevier Ltd; 2003. p. 20-23.
[14] Ertl F. Pixel-perfect building with alignment to the pixel grid. Presentation; 2017.
[15] Lithoz GmbH. Thermal Post Processing – LithaLox 350, Data Sheet. Vienna; 2020.